Neutron-scattering studies of a phase transition in the metamagnet $FeBr_2$ under external magnetic fields

K. Katsumata and H. Aruga Katori
The Institute of Physical and Chemical Research (RIKEN), Wako, Saitama 351-01, Japan

S. M. Shapiro and G. Shirane
Physics Department, Brookhaven National Laboratory, Upton, New York 11973

(Received 7 October 1996)

Neutron-scattering experiments have been performed on the metamagnet $FeBr_2$ under external magnetic fields. We find an anomaly in the temperature (T) and magnetic-field (H) dependences of the intensity of the (2,0,1/2) antiferromagnetic Bragg scattering at the temperature $T_1(H)$ at which an anomaly in specific heat has been observed in addition to the anomaly at the Néel temperature $T_N(H)$. We argue that our results are consistent with the theoretical H-T phase diagram of a metamagnet in which the tricritical point decomposes into a critical end point and a bicritical end point. We locate the latter point at $T_{cr} \cong 10.8$ K and $H_{cr} \cong 1.4$ T in this compound. [S0163-1829(97)08317-3]

I. INTRODUCTION

Antiferromagnets with a strong uniaxial anisotropy exhibit a phase transition from a state with very small net moment to the saturated paramagnetic state under an applied magnetic field at low temperatures. This field-induced phase transition (metamagnetic transition) has been studied for more than 50 years.[1] The magnetic-field–temperature (H-T) phase diagram of a metamagnet is shown schematically in Fig. 1(a). The solid line represents a first-order transition and the dotted one a second-order transition which meet at a tricritical point (TCP). The existence of this H-T phase diagram has been confirmed theoretically[1] and a number of substances exhibiting this phase diagram has been found.[1,2] A decomposition of TCP into a critical end point (CEP) and a bicritical end point (BCEP), shown schematically in Fig. 1(b), has been predicted by a mean-field theory[3] and a Monte Carlo simulation,[4] when a further-neighbor interaction is introduced in addition to the nearest-neighbor one in the former case and when a single ion anisotropy term is included in the latter case. On the other hand, a Monte Carlo simulation[5] on a three-dimensional Ising antiferromagnet with next-nearest-neighbor interaction shows no evidence for a decomposition of a TCP into a CEP and BCEP. The H-T phase diagram shown in Fig. 1(b) has attracted renewed theoretical interest[6–8] in recent years motivated by the discovery[9] of a new boundary in the H-T plane of the metamagnet $FeBr_2$.

The compound $FeBr_2$ has the hexagonal CdI_2 structure and exhibits an antiferromagnetic ordering below 14.2 K. In the ordered phase, spins in a c plane are parallel which are aligned antiparallel with spins in the adjacent planes along the c axis. The H-T phase diagram of $FeBr_2$ has been determined from magnetic measurements.[10,11] Qualitatively, the experimental phase diagram is similar to the one shown in Fig. 1(a) with a TCP at $T_t = 4.6$ K and $H_t = 2.88$ T. One important thing to be noted here is that the first- and second-order lines in $FeBr_2$ do not meet smoothly at the TCP as the simple theory tells. The second-order line in $FeBr_2$ shows a maximum above T_t and makes an angle with the first-order line at the multicritical point. This reminds us that the actual phase diagram of $FeBr_2$ is closer to the one shown in Fig. 1(b).

Recently, Azevedo *et al.*[9] have found two new boundaries in the H-T plane of $FeBr_2$, one above and the other below the second-order line. At these boundaries the temperature and magnetic field dependences of the imaginary part (χ'') of the ac susceptibility show an anomaly. These authors claimed that the anomalies originate from noncritical spin fluctuations. The results of Mössbauer spectroscopy[12] on $FeBr_2$ in external magnetic fields were interpreted based on a model that the external magnetic field induces a transversal precession of the moments on the down sublattice. Aruga Katori *et al.*[13] have measured the specific heat (C_p) of a single crystal of $FeBr_2$ under external magnetic fields. They found two anomalies in C_p for $1.4\ \text{T} \leqslant H \leqslant 2.9$ T and $T \geqslant 4.9$ K. The anomaly at the higher temperature represents the transition from the paramagnetic to antiferromagnetic phase. The anomaly at the lower temperature appears in the

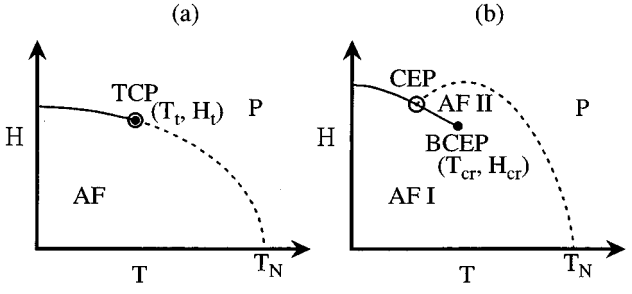

FIG. 1. (a) Magnetic field (H) vs temperature (T) phase diagram of a metamagnet. AF, antiferromagnetic phase; P, paramagnetic phase; TCP, tricritical point. The solid line represents a first-order transition and the dotted one a second-order transition. (b) A decomposition of the TCP into a critical end point (CEP) and a bicritical end point (BCEP) predicted by a mean-field theory.

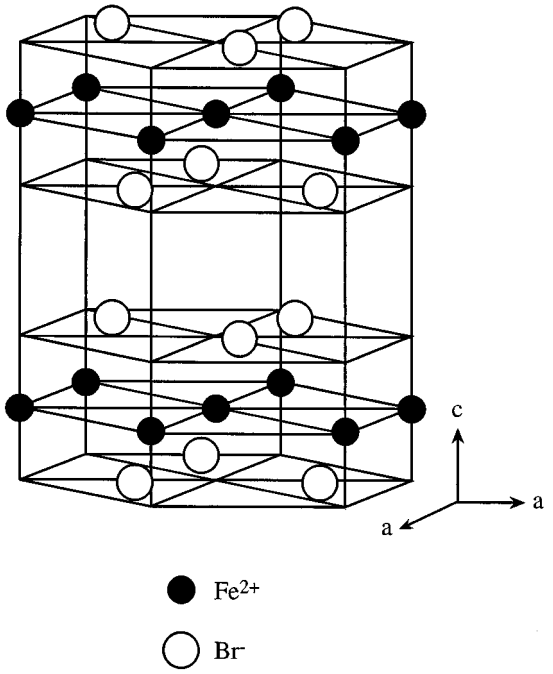

FIG. 2. Crystal structure of $FeBr_2$.

form of a peak superposed on a broad shoulder, indicating the occurrence of a phase transition at this boundary.

By Monte Carlo simulations, Selke and Dasgupta[6] were able to reproduce the two anomalies in the temperature dependence of both dM/dT (the derivative of dc magnetization with respect to temperature) and C_p in the applied magnetic field observed in $FeBr_2$. The physical origin of these anomalies originates from the interplay of the effectively weak coupling in the c plane and the coupling to several sites in adjacent c planes.[6,7] Starting from the infinite-dimensional Hubbard model with uniaxial anisotropy, Held *et al.*[8] have obtained the H-T phase diagram schematically shown in Fig. 1(b) which, they claim, is qualitatively very similar to the experimental phase diagram of $FeBr_2$.

In order to get a deeper understanding on the phase transition in $FeBr_2$, we have performed neutron-scattering experiments under applied magnetic fields. The neutron-scattering technique has an advantage over the other ones in that it measures directly the order parameter, thus providing us with an important information on the phase transition.

The format of this paper is as follows. In Sec. II the magnetic properties of $FeBr_2$ and relevant information are given. The experimental details are given in Sec. III. The experimental results are given in Sec. IV. The last section is devoted to a discussion.

II. PRELIMINARY DETAILS

The compound $FeBr_2$ has the hexagonal CdI_2 structure (D_{3d}^3) shown in Fig. 2. The structure consists of Fe^{2+} layers which are sandwiched by two Br^- bilayers along the c axis. The lattice constants at room temperature are $a=3.772$ Å and $c=6.223$ Å. From a specific heat measurement,[14] a magnetic ordering occurs at 14.2 K in zero field. The magnetic structure determined from neutron scattering[15] is such that spins in the c plane are parallel to each other with anti-

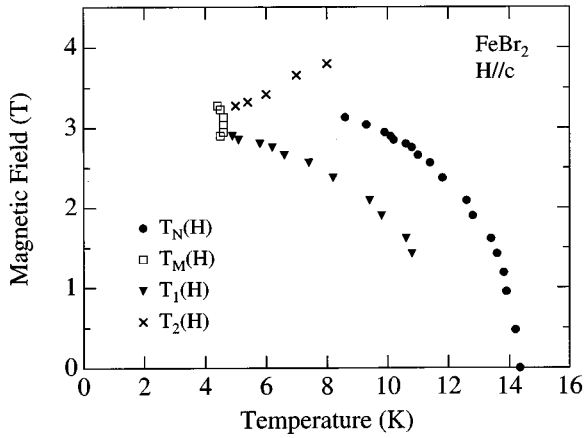

FIG. 3. The magnetic field (H) vs temperature (T) phase diagram of $FeBr_2$ determined from the specific heat measurements (Ref. 13). The magnetic field is applied parallel to the easy axis (c axis).

parallel alignment between the neighboring spins along the c axis.

The electronic ground state of Fe^{2+} in $FeBr_2$ is a triplet, the lowest excited state lying $\sim 100\ cm^{-1}$ above it. Thus, the effective Hamiltonian describing the low-temperature properties of $FeBr_2$ is written as[16]

$$\mathcal{H}=\sum_i D\{(S_i^z)^2-2/3\}$$

$$+\sum_{i>j}\{-(2/\eta)J_{ij}S_i^zS_j^z-2J_{ij}(S_i^xS_j^x+S_i^yS_j^y)\}, \quad (1)$$

with $S=1$. Here, D is the energy difference between the doublet and singlet in the lowest triplet, J_{ij} is the exchange interaction constant, and η is a constant describing the anisotropy in the exchange interactions. All the parameters in Eq. (1) have been determined from the neutron inelastic scattering study[16] to be

$$\begin{aligned} 2J_1&=0.152\ \text{THz},\\ 2J_2&=-0.051\ \text{THz},\\ 2J'&=-0.06\ \text{THz},\\ D&=-0.22\ \text{THz},\\ \eta&=0.78, \end{aligned} \quad (2)$$

where J_1 and J_2 are the nearest- and next-nearest-neighbor exchange interaction constants in the c plane, respectively, and J' is the exchange interaction constant between planes. As one can recognize, the first term in Eq. (1) has the form of a single-ion anisotropy with the easy axis along the z axis which is taken to be parallel to the c axis of the crystal. The value of D is larger than that of J' and this is the reason why $FeBr_2$ exhibits a metamagnetic transition.

Figure 3 shows the H-T phase diagram of $FeBr_2$ determined from the specific heat measurements.[13] In zero field, only one sharp anomaly in C_p was found at the Néel temperature (T_N) of 14.2 K being consistent with the previous work.[14] As H increases, T_N decreases. For $1.4\ \text{T}\leqslant H\leqslant 2.9$ T,

another anomaly in C_p appears in the form of a peak superposed on a broad shoulder. The peak becomes sharp with the increase of the magnetic field up to 2.9 T, which shows the existence of a new phase boundary. Below 1.4 T, it was unable to resolve the two anomalies. The H-T phase diagram shown in Fig. 3 is quantitatively the same as the one determined from the magnetic measurements.[9]

III. EXPERIMENTAL DETAILS

The single crystal of $FeBr_2$ was grown by the Bridgman technique. The powders of $FeBr_2$ were obtained by a direct reaction of Fe (Johnson Matthey, Specpure) with HBr gas (Matheson, 99.8%). After the reaction, the powders were packed into a quartz ampoule and heated up to 800 °C under a stream of HBr gas for a further purification. The dimensions of the single crystal used in this experiment were about 10 mm×15 mm×3 mm. The crystal consisted of a few domains.

The neutron-scattering experiments were carried out on the H4M triple-axis spectrometer at the High Flux Beam Reactor of the Brookhaven National Laboratory. The horizontal collimator sequence was 20′-40′-S-20′-80′. A pyrolytic graphite filter after the sample was used to eliminate higher-order beams. The phase diagram discussed above corresponds to the field applied along the c axis. Because of the antiparallel arrangement between neighboring spins along the c axis, the magnetic reflections all contain half integer Miller indices $l=(2n+1)/2$ (n an integer). The crystal is mounted in a flow cryostat inside a vertical superconducting magnet. In order to study the magnetic reflections with the field applied along the c axis, the crystal is tilted by $\sim 4°$ about the [110] direction within the cryomagnet, and so the c axis makes an angle of $\sim 4°$ with respect to the field direction. This slight tilting of the c axis does not alter the H-T phase diagram because the component of H parallel to the c axis is $\sim H\cos 4° = 0.998H$. This orientation allows us to study the (2,0,1/2) magnetic Bragg peak as well as the orthogonal (1,1,0) nuclear peak.

IV. EXPERIMENTAL RESULTS

Figure 4 shows the temperature dependence of the intensity (I) of the (2,0,1/2) antiferromagnetic Bragg scattering for different magnetic fields. Since the linewidth of the (2,0,1/2) scattering does not depend much on T nor H as shown in Fig. 5, we plot in Fig. 4 the peak intensity. The width is almost resolution limited. It is evident that the external field changes drastically the temperature dependence of the intensity.

In order to see the effects of magnetic fields on the temperature dependence of $I(2,0,1/2)$ more clearly, we plot in Fig. 6, $I(2,0,1/2)$ as a function of T scaled by the respective Néel temperature $[T_N(H)]$ in applied magnetic fields obtained from the specific heat measurement.[13] At low fields ($H \leqslant 1.0$ T) the temperature dependence of $I(2,0,1/2)$ shows the behavior typical of an antiferromagnet in which I depends on the square of the sublattice magnetization. At high fields ($H > 1.50$ T), however, the data do not lie on the typical curve below about $T/T_N(H)=0.95$ and I depends almost

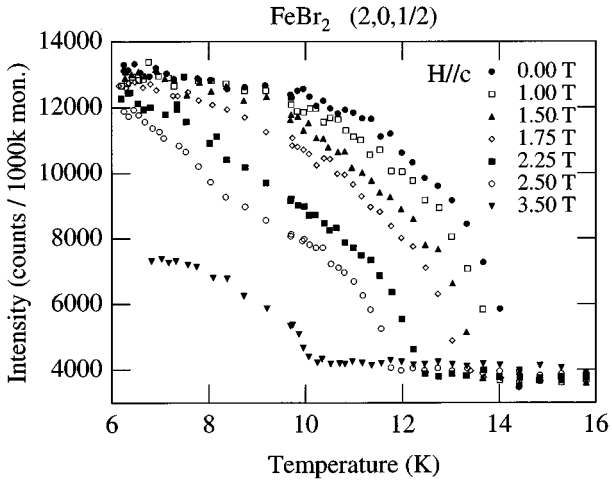

FIG. 4. Peak intensity at (2,0,1/2) vs temperature for different magnetic fields.

linearly on $T/T_N(H)$ above 2.25 T. These results suggest that we have another phase transition in addition to the one at $T_N(H)$ in the high-field region: If we had only one phase transition, all the data points measured in different fields should lie on a universal curve when the temperature is scaled with $T_N(H)$.

We show, in Fig. 7, $I(2,0,1/2)$ versus T scaled by the temperature $[T_1(H)]$ at which an anomaly in specific heat has been observed[13] for $H=1.75$ T, 2.25 T, and 2.50 T. We see that the data points fall on a universal curve at low temperatures $T/T_1(H)<1$. On the other hand, they are not on a universal curve at high temperatures $T/T_1(H)>1$.

Figure 8 shows $I(2,0,1/2)$ versus H measured at the designated temperatures. Here, we subtracted the intensity at $T=20$ K as the background. In Fig. 9 is shown $I(2,0,1/2)$ as a function of H scaled by the critical field $[H(T_1)]$ at which an anomaly in C_p has been observed. The data points observed at low fields $H/H(T_1)<1$ fall on a universal curve. The data at high fields $H/H(T_1)>1$, on the other hand, are not on a universal curve.

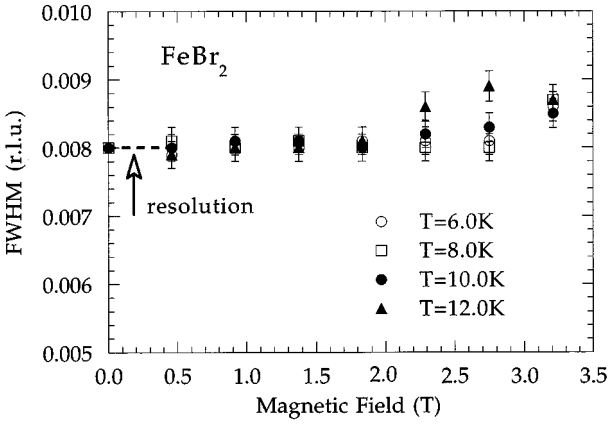

FIG. 5. Linewidth (full width at half maximum) vs magnetic field of the (2,0,1/2) magnetic Bragg peak measured along the [h 0 1/2] direction at several temperatures. The widths were obtained by Gaussian fits to the data.

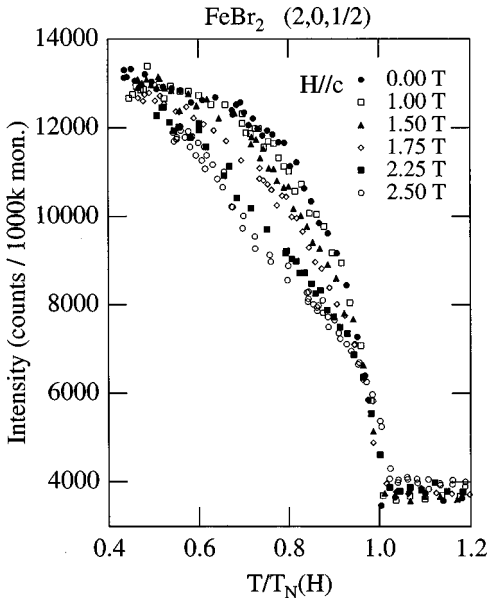

FIG. 6. Peak intensity at (2,0,1/2) vs reduced temperature $T/T_N(H)$. Here, $T_N(H)$ represents the Néel temperature in respective magnetic field determined from the specific heat measurements (Fig. 3).

V. DISCUSSION AND CONCLUSIONS

From Fig. 6, we see that all the data measured in different fields lie on a universal curve above about $T/T_N(H)=0.95$. This means that the character of the transition from the paramagnetic to antiferromagnetic phase does not change with H. The transition which is of second order occurs at the phase boundary denoted by $T_N(H)$ in Fig. 3.

From Fig. 7, we see that $I(2,0,1/2)$ measured at the designated fields changes with temperature in two steps indicating the existence of a boundary around $T/T_1(H)=1$. Figure 9 gives further evidence for the existence of the boundary at $H(T_1)$ or equivalently at $T_1(H)$ where the intensity changes abruptly.

Selke[7] has predicted from the mean-field calculation on a simple cubic Ising model that there exist two lines called

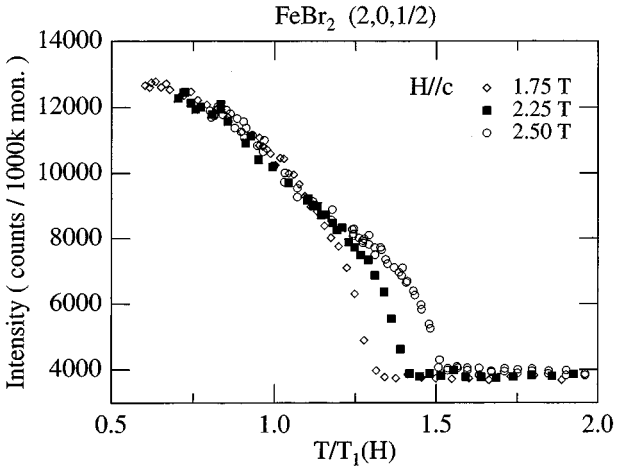

FIG. 7. Peak intensity at (2,0,1/2) vs reduced temperature $T/T_1(H)$. Here, $T_1(H)$ is the temperature at which an anomaly in specific heat has been observed (Fig. 3).

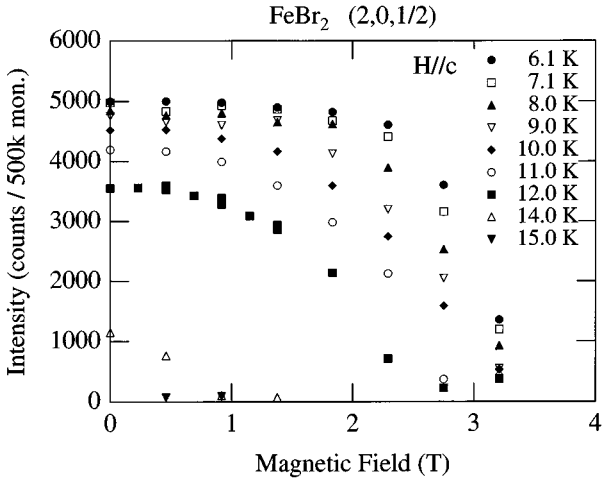

FIG. 8. Peak intensity at (2,0,1/2) vs magnetic field applied along the c axis for different temperatures.

T_T and T_H in the H-T phase diagram, which emerge from the bicritical end point. At T_T the temperature dependence of dM/dT shows an anomaly for fixed H. On the other hand, the field dependence of dM/dH shows an anomaly at T_H for fixed T. Also, the field dependence of the staggered magnetization exhibits an anomaly at T_H.[7] The results of the magnetic measurements[9] show that the anomaly in χ'' (and probably an anomaly in dM/dT) occurs at $T_1(H)$ in Fig. 3 at which an anomaly in C_p has also been observed. Figure 9 shows that an anomaly in the staggered magnetization, which is proportional to the square root of $I(2,0,1/2)$, appears at $H(T_1)$ or, equivalently, at $T_1(H)$. These facts indicate that either the lines T_T and T_H merge into the line $T_1(H)$ in Fig. 3 or they are absent in $FeBr_2$.

Based on the former idea, the line $T_1(H)$ is not a true phase transition line but represents the positions at which noncritical spin fluctuations occur.[9] However, a sharp anomaly in C_p has been observed at $T_1(H)$ in high fields,[13] indicating the occurrence of a phase transition at this boundary. Based on the latter idea, we see close similarity of the

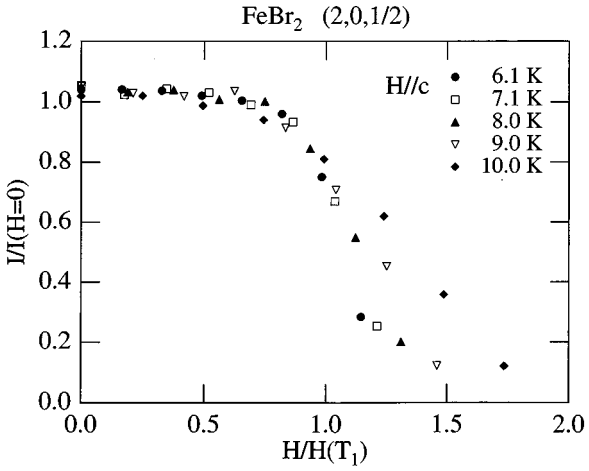

FIG. 9. Reduced peak intensity at (2,0,1/2) vs reduced magnetic field $H/H(T_1)$ for the designated temperatures. Here, $I(H=0)$ is the peak intensity at (2,0,1/2) measured in zero field and $H(T_1)$ is the magnetic field giving an anomaly in specific heat at T_1 (Fig. 3).

experimental H-T phase diagram shown in Fig. 3 to the theoretical one shown in Fig. 1(b).

We call the layers with positive magnetic moments (// H) the + layers and the ones with negative moments the − layers. In zero field, the magnetization (m_+) in the + layers and that in the − layers (m_-) are oppositely directed and their magnitudes are equal. For finite H, in the AF I phase of Fig. 1(b), $m_+ > m_-$ yet they are oppositely directed. On the other hand, in the AF II phase, $m_+ \neq m_-$ and they are parallel.[7] In the region $H < H_{cr}$, where H_{cr} is the BCEP field, the transition between the AF I and AF II phases is continuous. This is consistent with the result shown in Fig. 6 in which only one anomaly in the temperature dependence of $I(2,0,1/2)$ has been observed at $T_N(H)$ below about 1.5 T. This is also consistent with the fact that only one anomaly in C_p has been observed below about 1.4 T.[13] At high fields ($H > H_{cr}$), the transition from the AF I to AF II phase is expected to be of first order. Experimentally, no jump in sublattice magnetization is observed at $T_1(H)$ as shown in Fig. 7. This is probably due to demagnetization effects which give rise to a region where the AF I and AF II phases coexist. A sharper change in the sublattice magnetization is observed at $H(T_1)$ when measurement is done under fixed temperatures (Fig. 9). This is understandable from the curvature of the $T_1(H)$ line in Fig. 3. The coexistence region is narrower along the H direction than along the T direction. From the above considerations, we conclude that the experimental H-T phase diagram of $FeBr_2$ is close to the one shown schematically in Fig. 1(b). We tentatively locate the bicritical end point at $T_{cr} \cong$ 10.8 K and $H_{cr} \cong$ 1.4 T based on the H-T phase diagram shown in Fig. 3.

In conclusion, we have studied the magnetic phase transition in the metamagnet $FeBr_2$ under external magnetic fields by the neutron-scattering technique. We find an anomaly in the temperature dependence of the intensity of the (2, 0, 1/2) antiferromagnetic Bragg scattering at $T_1(H)$ in addition to that at $T_N(H)$. We conclude that the H-T phase diagram is close to the one shown schematically in Fig. 1(b) with a BCEP located at $T_{cr} \cong$ 10.8 K and $H_{cr} \cong$ 1.4 T.

ACKNOWLEDGMENTS

This work was partially supported by the U.S.-Japan Cooperative Program on Neutron Scattering operated by the U.S. Department of Energy and the Japanese Ministry of Education, Science, Sports and Culture, by the Special Coordination Funds of the Science and Technology Agency of the Japanese Government, and by the NEDO International Joint Research Grant. Work at Brookhaven National Laboratory was carried out under Contract No. DE-AC02-76CH00016, Division of Materials Science, U.S. DOE.

[1] For a review see J. M. Kincaid and E. G. D. Cohen, Phys. Rep. **22**, 57 (1975); E. Stryjewski and N. Giordano, Adv. Phys. **26**, 487 (1977).

[2] K. Katsumata, in *Magnetic Properties of Halides*, edited by H. P. J. Wijn, Landolt-Börnstein New Series, Group III, Vol. 27j1, pt. 9 (Springer-Verlag, Berlin, 1994), p. 1, and references therein.

[3] K. Motizuki, J. Phys. Soc. Jpn. **14**, 759 (1959).

[4] Y. L. Wang and J. D. Kimel, J. Appl. Phys. **69**, 6176 (1991).

[5] H. J. Herrmann and D. P. Landau, Phys. Rev. B **48**, 239 (1993).

[6] W. Selke and S. Dasgupta, J. Magn. Magn. Mater. **147**, L245 (1995).

[7] W. Selke, Z. Phys. B **101**, 145 (1996).

[8] K. Held, M. Ulmke, and D. Vollhardt, Mod. Phys. Lett. **10B**, 203 (1996).

[9] M. M. P. de Azevedo, Ch. Binek, J. Kushauer, W. Kleemann, and D. Bertrand, J. Magn. Magn. Mater. **140-144**, 1557 (1995).

[10] A. R. Fert, P. Carrara, M. C. Lanusse, G. Mischler, and J. P. Redoules, J. Phys. Chem. Solids **34**, 223 (1973).

[11] C. Vettier, H. L. Alberts, and D. Bloch, Phys. Rev. Lett. **31**, 1414 (1973).

[12] J. Pelloth, R. A. Brand, S. Takele, M. M. P. de Azevedo, W. Kleemann, Ch. Binek, J. Kushauer, and D. Bertrand, Phys. Rev. B **52**, 15 372 (1995).

[13] H. Aruga Katori, K. Katsumata, and M. Katori, Phys. Rev. B **54**, R9620 (1996).

[14] M. C. Lanusse, P. Carrara, A. R. Fert, G. Mischler, and J. P. Redoulés, J. Phys. (Paris) **33**, 429 (1972).

[15] M. K. Wilkinson, J. W. Cable, E. O. Wollan, and W. C. Koehler, Phys. Rev. **113**, 497 (1959).

[16] W. B. Yelon and C. Vettier, J. Phys. C **8**, 2760 (1975).